APSB
Acta Pharmaceutica Sinica B

2020
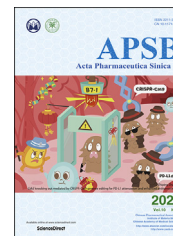
ORIGINAL ARTICLE

PCC0208017, a novel small-molecule inhibitor of MARK3/MARK4, suppresses glioma progression *in vitro* and *in vivo*

Fangfang Li[a], Zongliang Liu[a], Heyuan Sun[a], Chunmei Li[a], Wenyan Wang[a], Liang Ye[b], Chunhong Yan[a,c], Jingwei Tian[a,*], Hongbo Wang[a,*]

[a]*School of Pharmacy, Key Laboratory of Molecular Pharmacology and Drug Evaluation (Yantai University), Ministry of Education, Collaborative Innovation Center of Advanced Drug Delivery System and Biotech Drugs in Universities of Shandong, Yantai University, Yantai 264005, China*
[b]*Department of Clinical Medicine, Binzhou Medical College, Yantai 256603, China*
[c]*GRU Cancer Center, Augusta University, Augusta, GA 30912, USA*

Abstract   Gliomas are the most common primary intracranial neoplasms among all brain malignancies, and the microtubule affinity regulating kinases (MARKs) have become potential drug targets for glioma. Here, we report a novel dual small-molecule inhibitor of MARK3 and MARK4, designated as PCC0208017. *In vitro*, PCC0208017 strongly inhibited kinase activity against MARK3 and MARK4, and strongly reduced proliferation in three glioma cell lines. This compound attenuated glioma cell migration, glioma cell invasion, and angiogenesis. Molecular mechanism studies revealed that PCC0208017 decreased the phosphorylation of Tau, disrupted microtubule dynamics, and induced a G2/M phase cell cycle arrest. In an *in vivo* glioma model, PCC0208017 showed robust anti-tumor activity, blood−brain barrier permeability, and a good oral pharmacokinetic profile. Molecular docking studies showed that PCC0208017 exhibited high binding affinity to MARK3 and MARK4. Taken together, our study describes for the first time that PCC0208017, a novel MARK3/MARK4 inhibitor, might be a promising lead compound for treatment of glioma.

*Corresponding authors. Tel./fax: +86 535 6706060.
E-mail addresses: YTUpharmlab@163.com (Jingwei Tian), hongbowangyt@gmail.com (Hongbo Wang).

1. Introduction

Gliomas, the most common primary intracranial neoplasms in adults, are associated with the highest mortality and morbidity rates among all brain malignancies[1]. The rapid proliferation and high aggressiveness of gliomas contribute to the poor prognosis in patients, with a median survival time of approximately 14.6 months[2]. Currently, temozolomide (TMZ) is the most commonly used chemotherapeutic drug as a first-line agent for newly diagnosed gliomas. However, the associated toxicity and ensuing drug resistance to TMZ limits its efficacy and clinical use. Therefore, the identification of new agents based on novel targets is critical to bring benefit to glioma patients and improve treatment.

Microtubule-affinity regulating kinases (MARKs) are novel mammalian serine/threonine kinases that phosphorylate microtubule associated proteins (MAPs), such as Tau, and regulate cell cycle progression and cytoskeletal dynamics. Four MARK isoforms have been identified in humans (MARK1, MARK2, MARK3 and MARK4)[3,4], and all are highly enriched in human brain[5]. The four isoforms share a similar structural organization: one N-terminal header, a kinase domain, a ubiquitin-associated domain, a spacer region, and a kinase-associated domain[6,7]. Recent studies have shown that MARKs play important roles during the development and progression of cancer. MARK1 is implicated in cell migration in cervical tumor cells[8]. MARK2 overexpression has been identified in cisplatin-resistant non-small cell lung cancer[9]. MARK3 is overexpressed in human hepatocellular carcinoma and proposed to play a role in hepatocellular carcinogenesis by acting as a messenger in the WNT signaling pathway[10]. The MARK4 gene is duplicated and upregulated in glioblastomas[11,12] and also exhibits important functions in prostate cancer, breast cancer, hepatocarcinoma and leukemia cell lines[10,13−15]. Therefore, blocking the over-expression and/or over-activation of MARKs by small molecular inhibitors might be a potential therapeutic strategy against cancer. Therefore, a pan-MARKs inhibitor might be better anti-glioma drug *vs.* a highly selective inhibitor of a single MARK.

Based on the demonstrated functions of MARKs in cancer, many researches are ongoing for the development of MARK inhibitors. Only a few anti-MARK compounds have been described (*e.g.*, rutin and vanillin) and these agents were indeed found to suppress the growth of several cancer cells[16]. Recently, isatin-triazole hydrazones and 3-*N*-aryl substituted-2-heteroarylchromones were identified through structure screening as two new series of MARK4 inhibitors[17,18]. Currently, most inhibitors of MARKs have only been studied *in vitro*, possibly because of low bioavailability. As part of our continuing effort to discover novel anti-cancer agents against glioma, here we report a novel potent MARK3 and MARK4 dual inhibitor, designated as PCC0208017 (Scheme 1). This compound demonstrated robust anti-tumor activity against glioma *in vitro* and *in vivo* and showed an excellent oral pharmacokinetic profile with good blood−brain barrier permeability.

2. Materials and methods

2.1. Materials

PCC0208017, obtained as yellow powder, has the molecular formula $C_{19}H_{20}F_3N_7$ (MW 404.2). Purity of the compound used in the present study was shown to be higher than 98% by HPLC. TMZ was purchased from Aladdin Bio-Chem Technology (85822-93-1, Shanghai, China). PCC0208017 was dissolved in DMSO and stored at $-20\ ^{\circ}C$ for less than 1 month before use in *in vitro* experiments. Vehicle (DMSO) was used as a control in all experiments at a maximum concentration of 0.1%. For *in vivo* experiments, PCC0208017 and TMZ were suspended in a 0.5% (*w/v*) aqueous solution of methylcellulose and then diluted in saline immediately before administration.

2.2. Cell lines and animals

The glioma cell lines GL261, U87-MG, U251, C6, A172 and U118, as well as the human umbilical vein endothelial cells (HUVECs) were purchased from the cell bank of Chinese Academy of Sciences (Shanghai, China) and grown in Dulbecco's modified Eagle's medium (Gibco, Grand Island, NY, USA) supplemented with 10% foetal bovine serum (Sijiqing Biological Engineering Materials, Hangzhou, China), 100 U/mL penicillin and 100 mg/mL streptomycin at $37\ ^{\circ}C$ with 5% CO_2. All cells were harvested in the exponential growth phase for assays.

Six-to eight-week-old male C57BL/6 mice were purchased from Vital River Laboratory Animal Technology (Beijing, China). The animals were quarantined and habituated to the new environment for 7 days and maintained in a specific pathogen-free environment with free access to sterilized food and water. The animal room was maintained on a 12 h light/dark cycle at $21 \pm 5\ ^{\circ}C$ and $55 \pm 5\%$ relative humidity. All animal studies comply with the ARRIVE guidelines, and all of the experimental protocols were approved by the Experimentation Animal Research Committee of Yantai University (Yantai, China).

2.3. Kinase inhibition assay

Kinase kits containing Ser/Thr 21 (PV4535) and Ser/Thr 25 (PV5116) were purchased from Thermo Fisher Scientific (Waltham, MA, USA). The effect of PCC0208017 on the activity of MARK enzymes was evaluated using the Z'-LYTE™ screening protocol provided in the kit. Briefly, PCC0208017 was prepared at
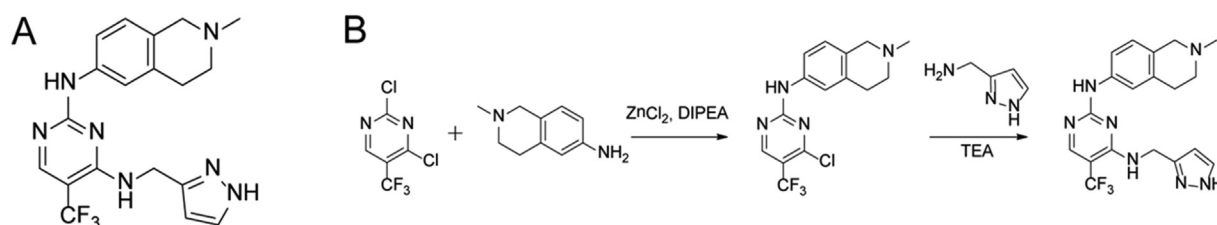
Scheme 1 The structure and the synthetic route of PCC0208017.

3-fold serial dilutions from the starting concentration and then 100 nL 100× test compound in 100% DMSO, 2.4 μL kinase buffer, 5 μL 2× peptide/kinase mixture and 2.5 μL 4× ATP solution were added in black 384-well plate (PV4514, Thermo Fisher Scientific). After shaking for 30 s, the plates were incubated for 1 h at room temperature. Five microliters of development reagent solution were added and the plate was shaken for another 30 s, followed by incubation for 1 h at room temperature. The plate was then read using a fluorescence plate reader and the data were analyzed. The effect of PCC0208001 on the activity of 18 common oncogenic kinases (purchased from Invitrogen, Carlsbad, CA, USA) was examined by ADP-GloTM at one concentration (100 nmol/L).

2.4. Cell viability assay

Cell viability was assessed using the MTT assay as previously reported[19]. Briefly, cells were plated into 96-well plates (2000−3000/well) and incubated overnight. The cells were treated with media or compounds for 72 h and then the MTT was added into each well. After the medium was removed, DMSO was added and the plates were gently oscillated until the color reaction was completed. The plates were then read at OD_{570nm} using a Molecular Devices SpectraMax M5 (Sunnyvale, CA, USA), and the relative cell survival and IC_{50} were calculated.

2.5. Cell proliferation assay

Cell proliferation was examined by cell growth curve assay and clone formation assay. In brief, cells were seeded in 6-well plates and cultured overnight. Cells were then incubated with designated concentrations of PCC0208017. After 24 h of treatment, the inhibitor-containing medium was removed. For the cell growth curve assay, the cells were collected and the numbers were counted. Growth curves were generated from cell counts over 6 consecutive days. For the clone formation assay, the cell clones were fixed 2 weeks post-planting and stained with crystal violet solution and clones were counted.

2.6. Western blotting assay

Total protein was extracted from cells or the xenograft tumors, and examined by Western blot following our previous published protocols[20]. Briefly, cells were lysed in the RIPA buffer and centrifuged at 4 °C. Equal amounts of protein (20−35 μg) were separated with SDS−PAGE and transferred onto PVDF membranes. Membranes were blocked and then incubated overnight with primary antibodies: MARK1 (#3319, Cell Signaling, Danvers, MA, USA), MARK2 (#9118, Cell Signaling), MARK4 (#4834, Cell Signaling), MARK3 (#9311, Cell Signaling), Tau (ab64193, Abcom, Cambridge, UK), p-Tau (ab92627, Abcom), and Cleaved-caspase 3 (#9661, Cell Signaling). After washes, the membranes were incubated with secondary antibodies. The immunoreactive bands were visualized using BeyoECL Plus purchased from Beyotime Institute of Biotechnology (Nantong, China) by enhanced chemiluminescence system (Pittsburgh, PA, USA).

2.7. Immunofluorescence assay

The effects of PCC0208017 on microtubule morphology were visualized by immunofluorescence microscopy following our previously published protocol[21]. Briefly, cells were plated into the 6-well plates coated with a cover slip and treated with PCC0208017 for 24 h. After fixing, permeabilizing, and blocking, the cells were incubated with monoclonal anti-β-tubulin-FITC antibody (F2043, Sigma−Aldrich, St. Louis, MO, USA) overnight at 4 °C. After washing, the cell nuclei were stained with Hoechst 33258 (C0003, Beyotime), and visualized using a confocal microscope (TCS SP8, Leica, Wetzlar, Germany).

2.8. Flow cytometry assay

Cell cycle analysis was performed using flow cytometry following our previously published protocol[22]. Briefly, the GL261 cells were seeded into 6-well plates with a density of 2×10^5 cells/well to adhere overnight, followed by treatment with various concentrations of PCC0208017 for 24, 48 or 72 h. The effects of PCC0208017 on cell cycle progression and apoptosis were determined using fluorescence-activated cell sorting (FACS) analysis with PI or PI/FITC-labeled annexin stained cells according to the manufacturer's recommended procedures and analyzed by a flow cytometer (BD Biosciences, SanJose, CA, USA).

2.9. LDH release

LDH released in GL261 cells was determined using the LDH Cytotoxicity Assay Kit (C0017, Beyotime) according to the manufacturer's instruction. Briefly, the cells were plated into 96-well plates and incubated overnight. The cells were treated with media or compounds and then the LDH solution was added into each well. The intensity of which was measured at 490 nm by a Molecular Devices SpectraMax M5 (Sunnyvale, CA, USA). The percentage cytotoxicity expressed as percent release of LDH was determined relative to controls as described by the manufacturer.

2.10. Wound healing assay

Cell migration was assessed using a wound-healing assay[23]. Cells were seeded in 24-well plates with 6% FBS-containing media and cultured until reaching confluence. The wound was introduced by scraping the cell monolayer with a sterile 200 μL pipette tips, and the cells were treated with the indicated concentrations of PCC0208017. After 0 and 18 h, the wound areas were quantified by measuring the width of the cell-free zone at six distinct positions with a digitally calibrated micrometer by microphotographs at 10× magnification, taken with OLYMPUS IX 73 inverted microscope equipped with a CCD camera.

2.11. Transwell assays

Transwell migration assays were performed using 6-well Transwell chambers (3428, Corning, NY, USA) containing 8 μm permeable pores according to the manufacturer's instructions. Cells in serum-free medium were seeded in the top chamber in the presence of indicated compounds, and the lower chamber was filled with complete medium. The cells were allowed to migrate

for 24 h and then the cells in the upper surface of membrane were carefully washed using PBS and removed with a cotton swab. The cells on the bottom part of membrane were fixed and stained with crystal violet, and the stained cells were visualized and counted from 6 randomly selected fields using a fluorescent inverted microscope. Directional migration was quantified by cell counting using Image J (NIH, Bethesda, MA, USA).

2.12. In vitro tube formation assay

The spontaneous formation of capillary-like structures *in vitro* on standard Matrigel was conducted following our previous protocol[22]. Briefly, a 96-well plate was coated with 50 μL Matrigel matrix (356234, Corning) for 30 min at 37 °C. After serum starvation for 6 h, HUVECs (2×10^4 cells/well) were seeded on the Matrigel bed and treated with PCC0208017 at the indicated concentration containing 10 ng/mL VEGF (293-VE, R&D System, Minneapolis, MN, USA). After 18 h, tube formations were recorded with an inverted microscope and the tubular structures were counted manually.

2.13. siRNA transfection

siRNA were provided from Genepharma (Shanghai, China) and used to transfect cells according to our previous protocol[24]. Briefly, cells seeded in 6-well plates were transfected with siRNA (80 pmol) using Lipofectamine 3000 (L3000015, Thermo Fisher Scientific), and the silencing efficiency was examined using Western blot assay 48 h after transfection. Negative control cells were transfected with *siLuc*. siRNA sequences targeting *MARK3* and *MARK4* were 5′-GGAGGAUGAGCUUAAGCCAUUUGUU-3′ and 5′-GCUGUACUCUCGAGCAAAU-3′, respectively. The *si-Luc* sequence is 5′- UUGUACUACACAAAAGUACUG-3′.

2.14. Xenograft tumors model

The xenograft tumors of murine glioma GL261 cells were established in C57BL/6 mice following our previous publication[25]. Briefly, cells (around 3×10^6 in 0.1 mL) were subcutaneously implanted into the left scapula of C57BL/6 mice ($n = 35$). When the tumors size reached approximately 100−300 mm³, the mice were randomized into five groups ($n = 7$/group): (a) control; (b) 100 mg/kg TMZ; (c) 100 mg/kg PCC0208017; (d) 50 mg/kg PCC0208017; and (e) 50 mg/kg PCC0208017+100 mg/kg TMZ. The control group was orally administrated with 0.5% methyl-cellulose solution every day. TMZ was orally administrated every 2 days and PCC0208017 was dosed every day at a volume of 10 mL/kg according to the animal's body weight. At the end of experiment, the mice were euthanized and the xenograft tumors were weighed.

2.15. Immunohistochemistry

The expression of CD31 in the xenograft tumors of GL261 was determined by immunohistochemical analysis. The samples were fixed in paraformaldehyde, dehydrated, and embedded in paraffin. The sections (4 μm) were processed for immunohistochemical staining as described previously[26]. Briefly, sections were blocked with 3% normal goat serum and incubated with antibodies against CD31 (1:200, #77699, Cell Signaling) overnight at 4 °C and then incubated with biotinylated secondary antibody, followed by avidin−biotin−peroxidase complex. Immunoreactivity signals were developed, and protein-positive cells were stained brown. Sections were examined under high-power microscopy (200×) using the Vectra automated quantitative pathology imaging system (PerkinElmer, Waltham, MA, USA).

2.16. Pharmacokinetic study

The primary pharmacokinetics profile of PCC0208017 was explored using C57BL/6 mice after a single oral administration at a dose of 50 mg/kg, the efficacy dosage in the above experiment. Briefly, 0.3 mL blood, as well as the brain tissues, was collected at pre-dose and 0.083, 0.167, 0.5, 1, 2, 4, 6, 8, 12, 24 and 36 h post-dose. Plasma was prepared after centrifugation at $6000 \times g$ for 5 min and then stored at −20 °C. The brain tissues were homogenized with saline (1:4, *w/v*). The concentration of PCC0208017 in the plasma samples and brain tissues were determined using LC−MS/MS system consisting of Agilent 1100 and TSQ Quantum Access (Thermo Electron Corporation, San Jose, CA, USA).

2.17. Molecular docking

The docking study was performed by CDOCKER module implemented in Discovery Studio (DS) 3.0. The crystal structures of MARK3 (PDB ID: 2QNJ) and MARK4 (PDB ID: 5ES1) downloaded from the protein data bank (PDB) were used for molecular docking. The structures were prepared by "Prepare Protein" module in DS with parameters kept as default. The water molecules were removed. The 3D structure of small molecule was prepared and minimized using "Prepare Ligands" and "Minimize Ligands" modules in DS, respectively. The binding site of MARK4 was defined by selecting residues around the native ligand in 5ES1 (in 7.5 Å radius). MARK3 was first aligned onto MARK4 and then the residues located in the binding site of MARK4 were defined as the binding site. Molecular docking was performed using "Docking Ligands (CDOCKER)" module. All the parameters were kept as default. The visualization of the docking results is shown in DS.

2.18. Statistical analysis

Data are presented as mean ± SD. *P* values were calculated by Dunnett of One-Way ANOVA using Graphpad (La Jolla, CA, USA), and $P < 0.05$ was considered statistically significant. The number of replicates and independent experiments is indicated in the figure legends.

3. Results

3.1. Synthesis of PCC0208017

The synthesis procedure of PCC0208017 is summarized as follows: zinc chloride was added to a solution of 2,4-dichloro-5-(trifluoromethyl) pyrimidine in DCE:*t*-BuOH (1:1, *v/v*) with ice cooling. The resulting solution was stirred and 2-methyl-1,2,3,4-tetrahydroisoquinolin-6-amine was added, followed by addition of a solution of DIPEA in DCE:*t*-BuOH (1:1, *v/v*). The crude product was purified by column chromatography to give N-(4-chloro-5-(trifluoromethyl)pyrimidin-2-yl)-2-methyl-

1,2,3,4-tetrahydroisoquinolin-6-amine, which was then mixed with (1*H*-pyrazol-3-yl)methanamine and Et₃N in *n*-butanol. The solvent was evaporated under reduced pressure, and the crude product was then purified by column chromatography, in which PCC0208017 was gained. The compound structure was confirmed by ¹H NMR (Supporting Information Fig. S1A) and ¹³C NMR (Fig. S1B).

3.2. PCC0208017 is predicted to bind with MARK3 and MARK4

Docking results of PCC0208017 are shown in Fig. 1. The compound could locate in binding site of MARK3 (Fig. 1A and B). The pyrimidine moiety of PCC0208017 played an important role in the interaction with MARK3 by forming multiple hydrophobic interactions with Val70, Met132 and Ala195 in MARK3. In addition, Ile62, Val116, Leu185 and Val205 around the small molecule also contributed to the binding by hydrophobic interactions. The secondary amine contacted Asp196 through a hydrogen bond. The protonated N atom of the piperidine ring formed a strong salt bridge interaction with Glu139 and Asp142, thus much improved the intermolecular interaction, which showed similar functions in the intermolecular interactions compared to those in MARK3-small molecule interaction. Notably, the pyrazol ring also showed multiple interactions with MARK4 (Fig. 1C and D). The ring formed π−π stacking with Tyr134, while the NH group interacted with Ala135 through a hydrogen bond, and additional π−σ and alkyl interactions could also be observed between this moiety and Ile62 and Leu185, respectively. These results indicated that the pyrazol ring of the small molecule may contribute to the target selectivity (Fig. 1C and D).

3.3. PCC0208017 inhibits the activity of MARK3 and MARK4

Enzyme assays showed that PCC0208017 could inhibit the kinase activity of MARK3 and MARK4 in a dose-dependent manner (Fig. 2A). The IC₅₀ values (50% of ATPase activity inhibition) of
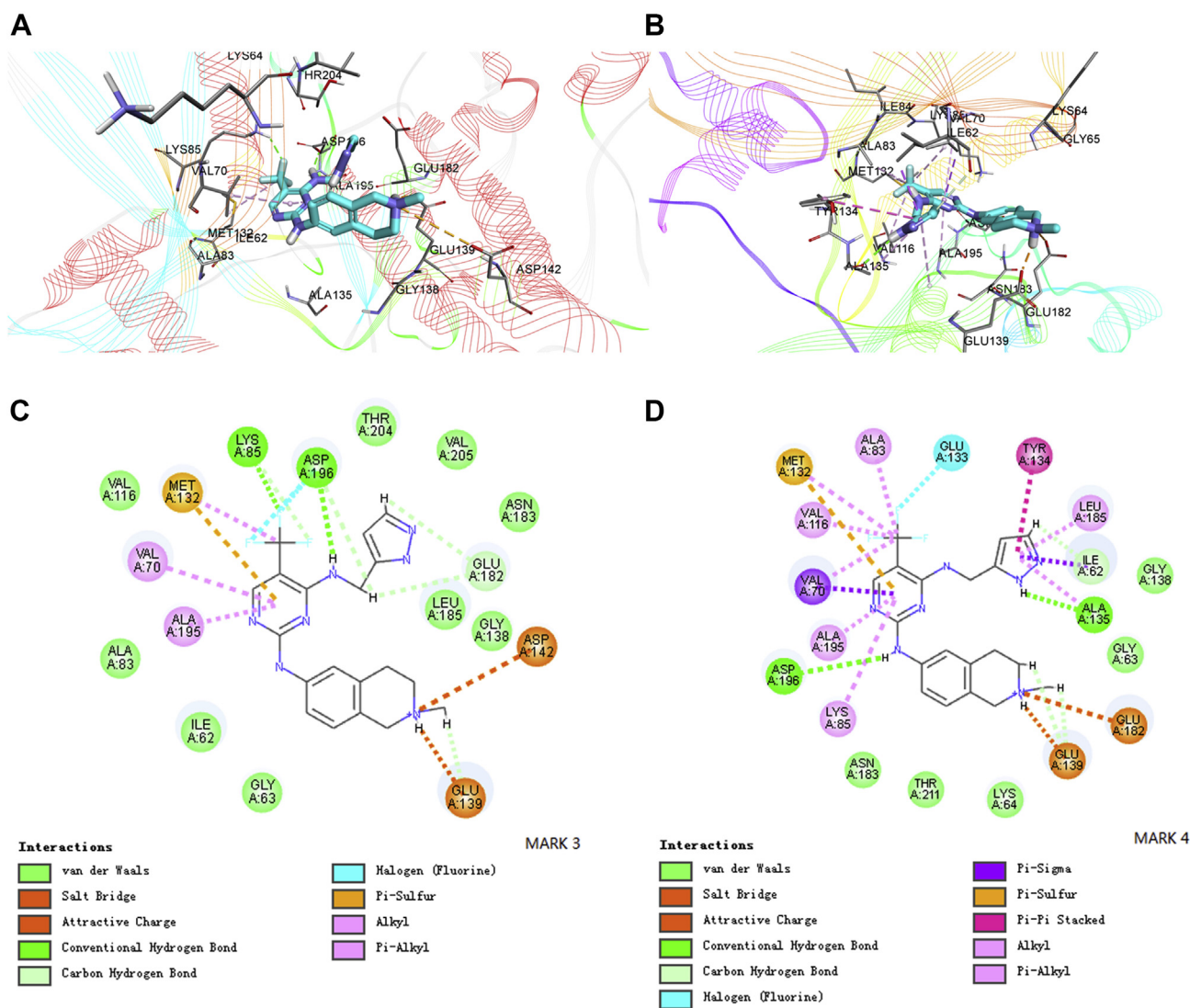
Figure 1 Binding of PCC0208017 with MARK3 and MARK4 were estimated by molecular docking. Upper panel (A, C) showes the pocket view of MARK3 and MARK4 binding with PCC0208017. Lower panel (B, D) showes the 2-dimensional schematic diagram of interactions of MARK3 and MARK4 with PCC0208017.
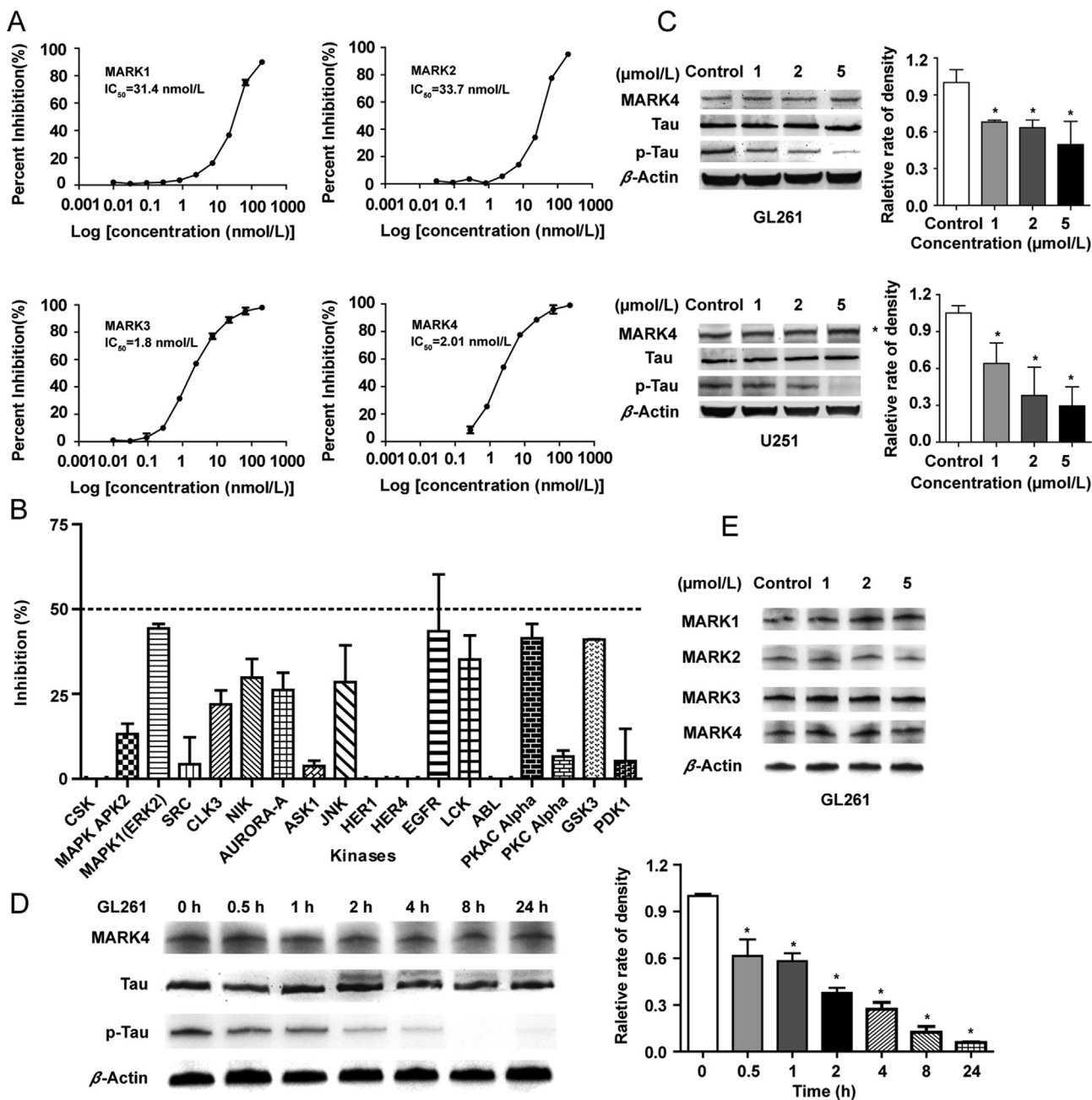
Figure 2 PCC0208017 inhibited the activity of MARK3 and MARK4 and decreased the phosphorylation of Tau. (A) The effects of PCC0208017 on the kinase activity of MARK1, MARK2, MARK3 and MARK4 were detected by commercial kit, and the IC_{50} was calculated. (B) The effect of PCC0208017 on the kinase activity of a panel of 18 oncogenic kinases (100 nmol/L). (C) The effects of PCC0208017 on the phosphorylation of Tau after 24 h treatment were detected by Western blot assay in GL261 and U251 cells. (D) The effects of PCC0208017 on the phosphorylation of Tau after different time treatment were detected by western blot assay in GL261. (E) The effects of PCC0208017 on the expression of MARK1, MARK2, MARK3 and MARK4 after 24 h treatment were detected by Western blot assay in GL261. Data represent mean ± SD of three different experiments. $^*P < 0.05$ compared with control group.

PCC0208017 against MARK3 and MARK4 were calculated as 1.8 and 2.01 nmol/L, respectively. Interestingly, PCC0208017 had much lower inhibitory activity against MARK1 and MARK2, with IC_{50} values of 31.4 and 33.7 nmol/L. No strong inhibitory activity was observed against 18 common oncogenic kinases (<50% inhibition) at 100 nmol/L (Fig. 2B). Consistent with these results, PCC0208017 treatment of GL261 and U251 cells, two commonly used glioma cell lines, resulted in decreased phosphorylation of Tau, the subtract of MARKs, with no impact on Tau steady state levels (Fig. 2C).

3.4. PCC0208017 suppresses the proliferation of glioma cells

We evaluated the expressions of MARK3 and MARK4 in several glioma cell lines using Western blot assay (Supporting
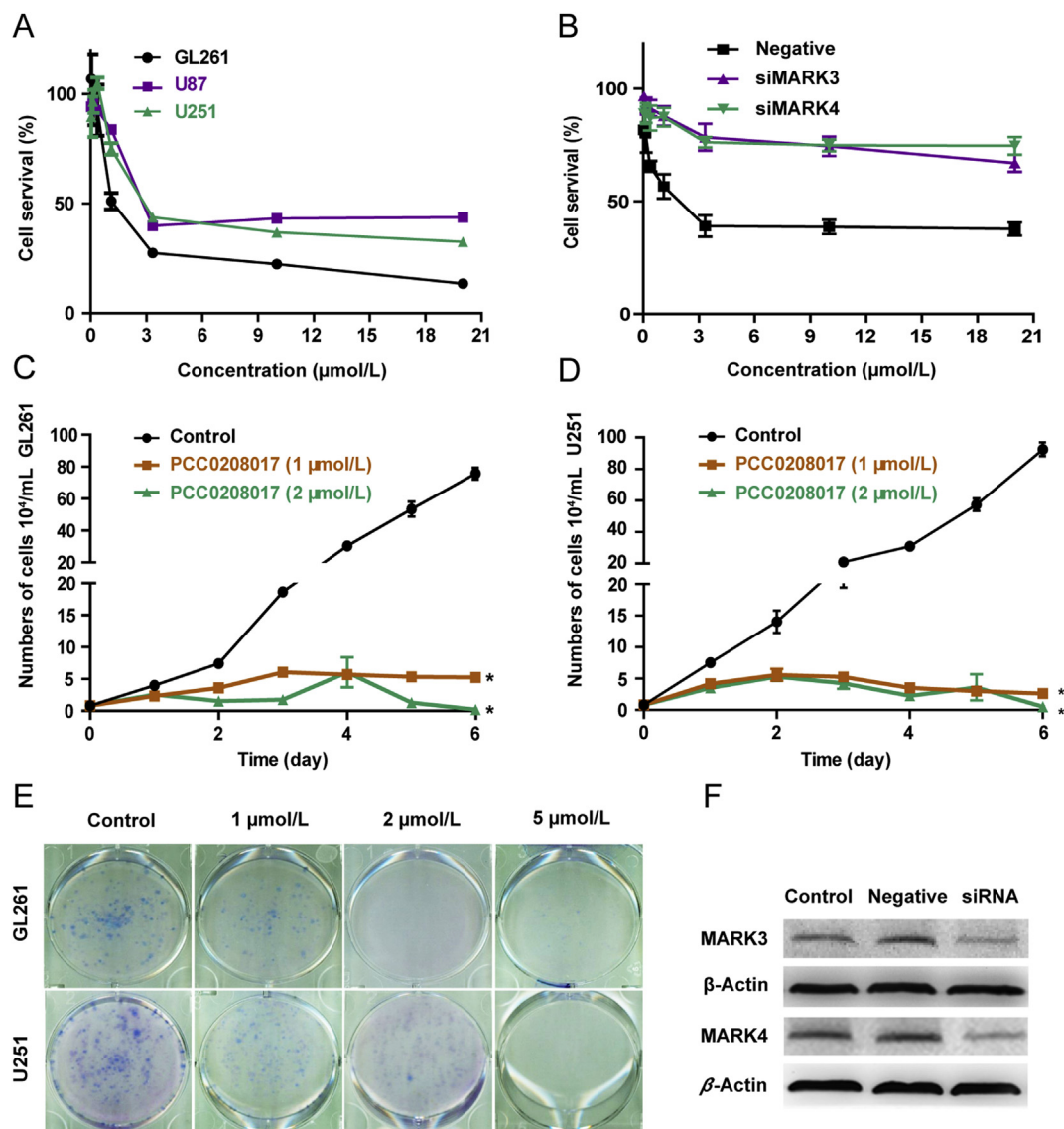
Figure 3 PCC0208017 inhibited glioma cells proliferation. GL261, U87-MG and U251 cells were exposed to various concentration of PCC0208017, and the cell proliferation determined by the MTT assay (A), the GL261 and U251 cell growth curve assay (C and D) and colony formation assay (E). The *MARK3* and *MARK4* were silenced by siRNA in U251 cells, in which the cells were performed for MTT assay (B) and the silence efficacy was detected by Western blot (F). Data represent mean $\pm$ SD of three different experiments. $^*P < 0.05$ compared with control group.

Information Fig. S2) and selected U87-MG, U251 and GL261 for subsequent cytotoxic activity study of PCC0208017. The results showed that PCC0208017 displayed cytotoxic activity against GL261, U87-MG and U251 cells (Fig. 3A), while the inhibitory effect was partially attenuated in U251 cells upon silencing for *MARK3* or *MARK4* (Fig. 3B and F). The IC$_{50}$ values of PCC0208017 for GL261, U87-MG and U251 were calculated as 2.77, 4.02 and 4.45 µmol/L, respectively. Consistent with these findings, both cell growth curves and colony formation assay showed that PCC0208017 decreased cell growth and colony forming ability in a dose-dependent manner (Fig. 3C, D and E). The LDH assays were also conducted and the results showed that LDH levels were increased in GL261 cells after treatment with PCC0208017 at 3 µmol/L for 72 h (Supporting Information Fig. S3).

3.5. PCC0208017 disrupts microtubule dynamics and induces G2/M phase cell cycle arrest and cell apoptosis

Based on the important role of MARKs in the regulation of microtubule dynamics, we examined the effects of PCC0208017 on microtubule morphology in glioma cells by immunofluorescence microscopy. Compared with the control group, GL261 cells treated with PCC0208017 for 24 h showed an increase in cell area and loss of cell polarity, the common phenotype of over-depolymerized microtubules (Fig. 4A). Microtubules are components of spindle fibers, which function in cell mitosis. To further determine whether the antiproliferative effects of PCC0208017 were associated with cell cycle arrest or apoptosis, flow cytometric analysis was performed.

Flow cytometry assays showed that the ratio of cells in G2/M phase significantly increased after 24, 48 and 72 h treatment with
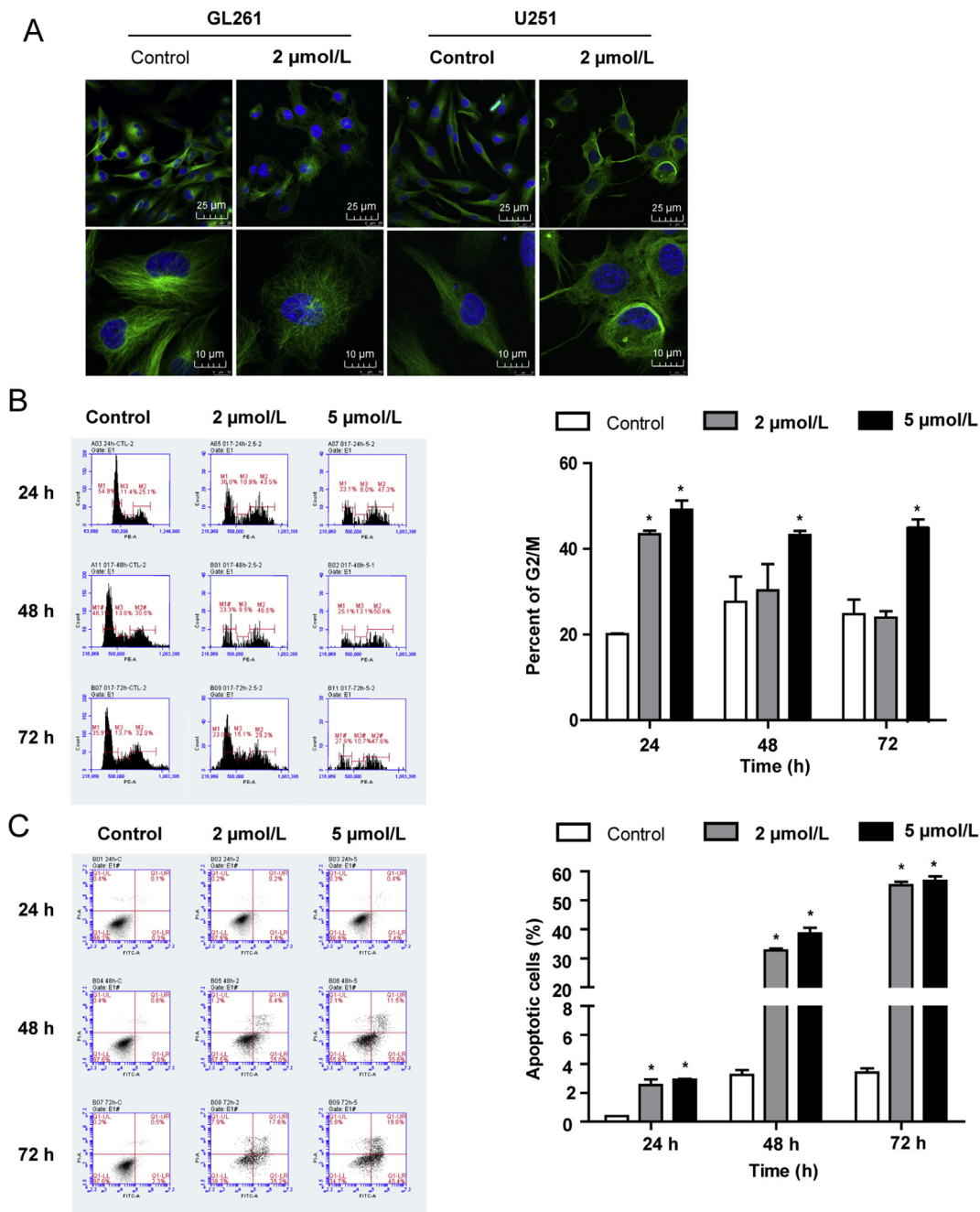
Figure 4 PCC0208017 changed microtubule dynamic, induced G2/M phase arrest and apoptosis in GL261 cells. Cells were treated with PCC0208017 for 24 h and then subjected to incubate with an anti-α-tubulin antibody and Hoechst 33258 to visualize the microtubule and nuclei. Images were examined by confocal and the representative pictures were taken (A). (Scale bar: 10 and 25 μm). GL261 cells treated with various concentrations of PCC0208017 for 24, 48 and 72 h were stained with PI for flow cytometry analysis (B). After treatments with various concentrations of PCC0208017 for 24, 48 and 72 h, GL261 cells were stained with annexin V−FITC and PI and then subjected to flow cytometry analysis (C). Data represent mean ± SD of three different experiments. $^*P < 0.05$ compared with control group.

PCC0208017 (Fig. 4B, $P < 0.05$ compared with the control group). At the same time, the cells after treatment with PCC0208017 were also observed undergoing apoptosis after staining with annexin V−fluorescein isothiocyanate (FITC) and propidium iodide (PI), in which the proportions of apoptotic cells increased from 2.8% to 59.4% in GL261 cells (Fig. 4C, $P < 0.05$ compared with the control group).

3.6. PCC0208017 suppresses cell migration and inhibits endothelial tube formation

As cell microtubule morphology changes are crucial for cell motility, we next performed wound-healing and Boyden chamber assays to evaluate the effect of PCC0208017 on the migration of glioma cells. At concentrations that exhibited minimal effects on

cell proliferation, PCC0208017 could significantly decrease cell migration and invasion (Fig. 5A and B, $P < 0.05$ compared with the control group). We also found that PCC0208017 at nontoxic concentrations could inhibit the HUVECs tube formation in a concentration-dependent manner (Fig. 5C, $P < 0.05$ compared with the control group).

3.7. PCC0208017 demonstrates robust antitumor activity in vivo and displays good BBB permeability

We next explored the *in vivo* anti-tumor activity of PCC0208017 in a xenograft glioma model. TMZ was used as the positive control. The results showed that PCC0208017 at dosages of 50 and 100 mg/kg could inhibit the growth of xenograft tumors derived from GL261 cells in a dose-dependent manner (Fig. 6B, $P < 0.05$ compared with the control group). Inhibition rates observed were 56.15% and 70.32%, respectively. Interestingly, co-treatment of PCC0208017 at dosage of 50 mg/kg could significantly enhance the anti-tumor activity of TMZ (Fig. 6B, $P < 0.05$ compared with the TMZ group), with an increase in tumor inhibition rates from 34.15% (TMZ only) to 83.5% (TMZ+PCC0208017). We also observed that the body weight in the animals treated with TMZ, but not PCC0208017, were

significantly decreased with controls (Fig. 6C, $P < 0.05$ *vs.* the control group), and co-treatment with PCC0208017 could significantly attenuate the TMZ-mediated decrease in animal body weight (Fig. 6C, $P < 0.05$ *vs.* the TMZ group). The immunohistochemistry assay showed that the expression of CD31 in the xenograft tumors was significantly decreased after treatment with PCC0208017 (Fig. 6E, $P < 0.05$ *vs.* control group).

In follow-up experiments, a preliminary pharmacokinetic study showed that PCC0208017 could be detected in both plasma and brain following a single oral dose of 50 mg/kg. In plasma, C_{max} was 1.36 μg/mL and T_{max} was 0.833 h. In brain, C_{max} was 0.14 μg/mL and T_{max} was 0.833 h (Fig. 7). These results were consistent with our previous design, demonstrating that the compound can be readily absorbed into the blood and distributed in brain.

4. Discussion

Gliomas are the most common malignant tumors among all intracranial tumors[27]. Currently, the identification of novel therapeutic agents based on new targets represents a major focus area of translational cancer research for glioma[28]. We report here for the first time that PCC0208017, a novel dual inhibitor of MARK3
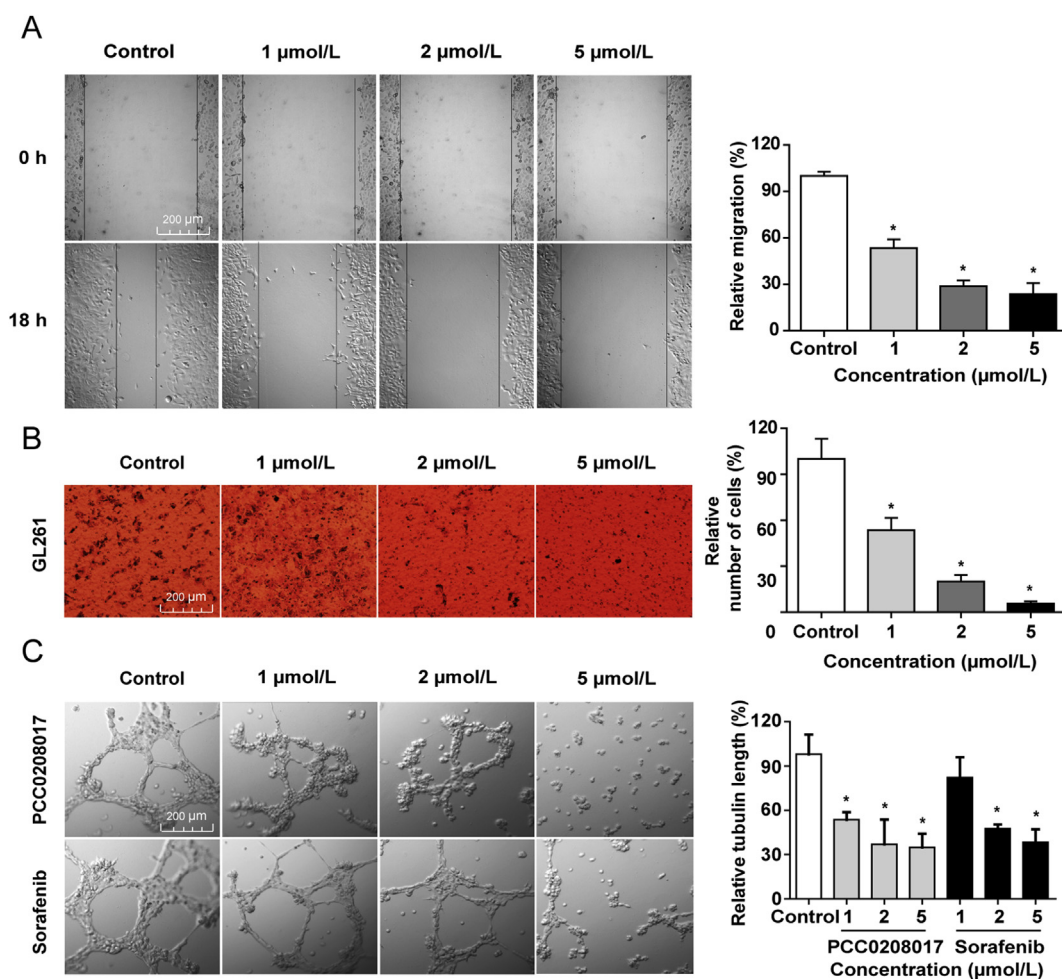
Figure 5 PCC0208017 inhibited GL261 cells migration and HUVECs tube formation. Cells were treated with test articles indicated before the cell wound-healing (A) and transwell migration assays (B) were performed or before the tube formation assay (C) was performed. Data represent mean ± SD of three different experiments. *$P < 0.05$ compared with control group. (Scale bar: 200 μm).
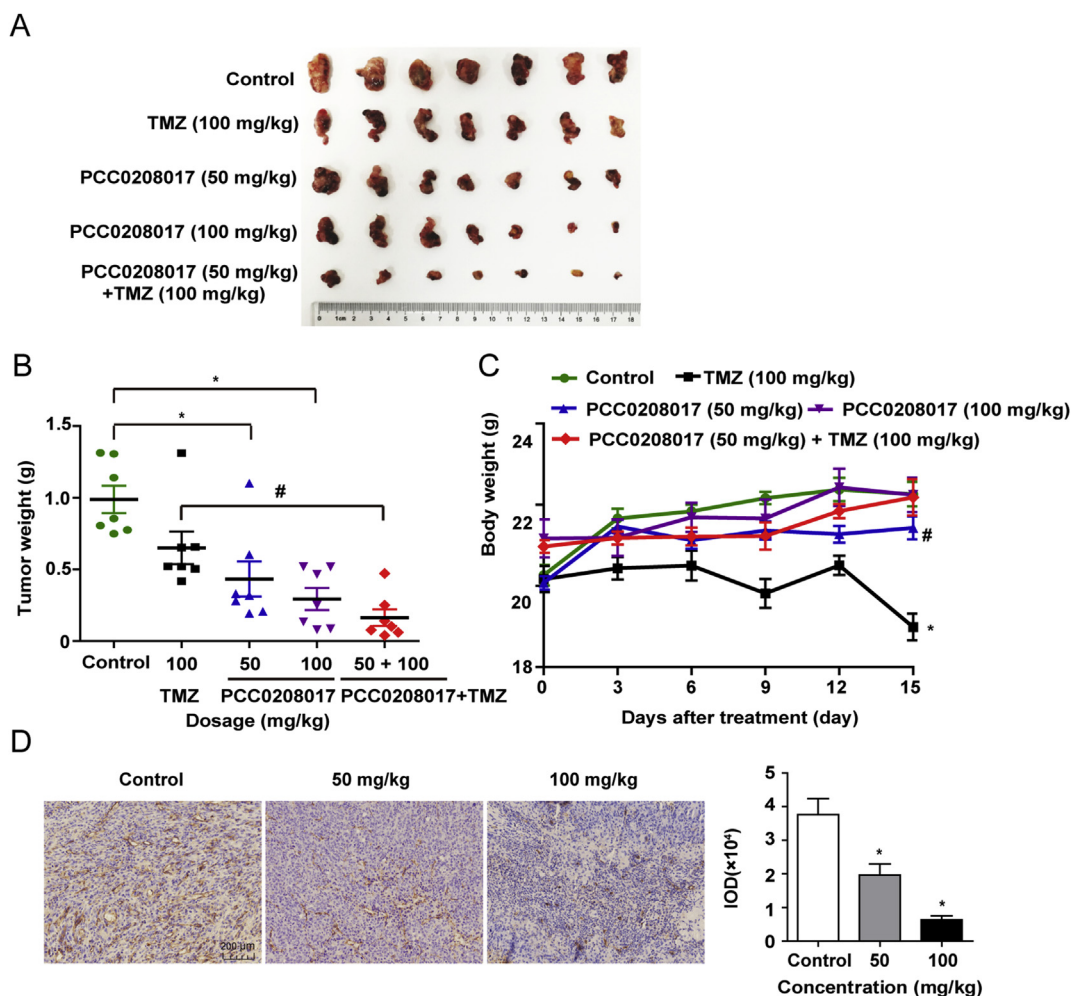
Figure 6 PCC0208017 inhibited GL261 cells growth in xenograft mouse model. Cells were transplanted in the C57BL/6 mice and treated with the tested articles indicated. The representative photographs of tumors after last treatment in each group were taken (A). Tumor weight (B) and body weight (C) were measured. (D) Immunohistochemically staining to evaluate the expression of CD31 (200×). Data represent mean ± SD of three different experiments. $^{*}P < 0.05$ compared with control group; $^{#}P < 0.05$ compared with TMZ group.

and MARK4, displayed robust anti-glioma activity *in vitro* and *in vivo*, with good *in vivo* pharmacokinetics prolife and blood−brain barrier permeability.

Microtubules and MAPs play critical roles in the cell cycle, and multiple studies have elucidated the regulatory mechanisms, including posttranslational modifications such as phosphorylation, that control their activities[29]. MARKs function as major protein kinases that phosphorylate MAPs, such as Tau, to regulate microtubules dynamics. Abnormal overexpression of MARKs has been linked with carcinogenesis of many malignant tumors, such as glioma, cervical cancer, non-small cell lung cancer, and liver cancer. Based on the evidence that the *MARK4* gene is upregulated in glioblastomas and its expression was positively correlated with the progression of glioma[12], MARK4 was recognized as a potential anti-cancer drug target. Indeed, PCC0208017 is able to inhibit the enzyme activity of both MARK3 and MARK4 with mild effects on MARK1 and MARK2. The selectivity towards MARK3 and MARK4 is likely due to its chemical design based on published MARK3 inhibitors[30,31]. At the same time, PCC0208017 showed only slight effect on other common oncogenic kinases, such as ABL and SRC, which would reduce the potential "on-target" related side effects. PCC0208017 could decrease the proliferation of selected glioma cells with high expression of MARK3

and MARK4, in which the mild inhibition of MARK1 and MARK2 might also contribute to cytotoxic activity. Consistent with our current findings, blockade of MARKs by inhibitors such as rutin or vanillin or using siRNA could suppress the growth of
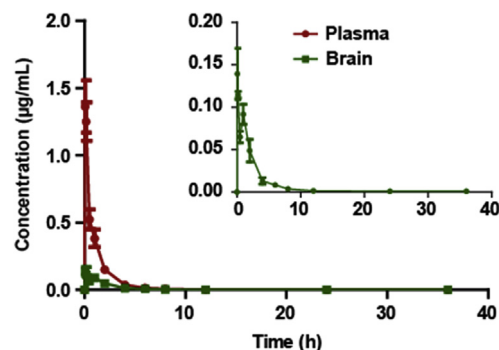
Figure 7 The primary pharmacokinetics profile of PCC0208017 following a single oral dose in C57BL/6 mice. PCC0208017 was suspended in a 0.5% methylcellulose solution and orally administrated to mice at a dose of 50 mg/kg, and the content of PCC0208017 in the plasma and brain tissues were quantified using LC−MS/MS system.

cancer cells (Supporting Information Fig. S5), indicated that inhibiting the activity of MARKs inhibits the survival of cancer cells expressing MARKs.

MARKs are microtubule-related affinity-regulated kinases that can affect the biological activity of substrates, such as Tau, *via* phosphorylation and regulate microtubule dynamics[32,33]. A previous study reported that MARK4 binds to the cellular microtubule network and centrosomes to regulate the cell cycle progression and cytoskeletal dynamics[34]. Our results showed that PCC0208017 decreased the phosphorylation of Tau and induced the depolymerization of microtubules, as indicated by cells with enlarged shape and without polarity. In addition, cells underwent a G2/M phase arrest, as well as the cell apoptosis after treatment with PCC0208017, which could also be observed in cells treated with microtubule-targeted anti-cancer drugs, such as paclitaxel and vincristine. We further found that PCC0208017 could decrease cell migration and invasion of glioma cells, as well as tube formation of HUVECs, a biomarker for the angiogenesis. This finding was in line with other reports, in which silencing *MARK4* using siRNA reduced the migration and invasion of breast cancer cells[14,15].

We further explored the *in vivo* anti-tumor activity of PCC0208017 using the classic xenograft model. Consistent with the *in vitro* findings, PCC0208017 indeed suppressed the growth of tumors derived from GL261 cells *in vivo* in a dose-dependent manner and displayed much less toxicity compared with TMZ, the first-line drug against glioma, at the equal therapeutic dosage, as indicated by changes in body weight. Interestingly, PCC0208017 could significantly potentiate the anti-tumor activity of TMZ, which might be because of its inhibitory against the angiogenesis, evidenced by the decreased CD31 expression in the xenograft tumors. Interestingly, PCC0208017 could attenuate the decrease in the body weight caused by TMZ, which indicated PCC0208017 might be used as a single agent or combined with TMZ-based chemotherapy regimens in the clinic. Currently, we did not know the reason for the separation of "synergism" and "detoxification" of PCC0208017 when combined with TMZ and the underlying mechanism supported for further investigation.

In treating malignant tumors within the central nervous system, the penetration of the blood−brain barrier by agents can be an obstacle to effectively deliver them into target regions. Thus this characteristic needs to be determined for all potential anti-glioma agents[35]. We found that PCC0208017 was detectable in the brain tissue after one orally-effective dose, indicating PCC0208017 showed good blood brain−barrier penetrability.

5. Conclusions

We report here for the first time that PCC0208017 suppresses the growth of glioma *in vitro* and *in vivo via* binding to and inhibiting MARK3 and MARK4. PCC0208017 also displayed a good oral pharmacokinetic profile and blood−brain barrier permeability. These results indicate that PCC0208017 might have the potential to be used as a single agent or an adjuvant therapy in combination with current chemotherapies against glioma.

Acknowledgments

Author contributions

Hongbo Wang, Jingwei Tian and Chunhong Yan designed the research. Fangfang Li, Zongliang Liu, Heyuan Sun, Chunmei Li, Wenyan Wang and Liang Ye performed experiments. Hongbo Wang, Fangfang Li and Wenyan Wang performed data analyses. Hongbo Wang and Jingwei Tian wrote the paper.

Conflicts of interest

The authors declare no conflicts of interest.

Appendix A.   Supporting information

Supporting data to this article can be found online at https://doi.org/10.1016/j.apsb.2019.09.004.

References

1. Daniel DA, Karim RF, William C, Beata D, Selby GC, H Gordon D, et al. Prognostic factors and survival in low grade gliomas of the spinal cord: a population-based analysis from 2006 to 2012. *J Clin Neurosci* 2018;**61**:14−21.
2. Ostrom QT, Gittleman H, Stetson L, Virk SM, Barnholtz-Sloan JS. Epidemiology of gliomas. *Cancer Treat Res* 2015;**163**:1−14.
3. Drewes G, Ebneth A, Preuss U, Mandelkow EM, Mandelkow E. MARK, a novel family of protein kinases that phosphorylate microtubule-associated proteins and trigger microtubule disruption. *Cell* 1997;**89**:297−308.
4. Trinczek B, Brajenovic M, Ebneth A, Drewes G. MARK4 is a novel microtubule-associated proteins/microtubule affinity-regulating kinase that binds to the cellular microtubule network and to centrosomes. *J Biol Chem* 2004;**279**:5915−23.
5. Timm T, Marx A, Panneerselvam S, Mandelkow E, Mandelkow EM. Structure and regulation of MARK, a kinase involved in abnormal phosphorylation of Tau protein. *BMC Neurosci* 2008;**9**:S9.
6. Bright NJ, Thornton C, Carling D. The regulation and function of mammalian AMPK-related kinases. *Acta Physiol* 2009;**196**:15−26.
7. Marx A, Nugoor C, Panneerselvam S, Mandelkow E. Structure and function of polarity-inducing kinase family MARK/Par-1 within the branch of AMPK/Snf1-related kinases. *FASEB J* 2010;**24**:1637−48.
8. Natalia MA, Alejandro GT, Virginia TJ, Alvarez-Salas LM. MARK1 is a novel target for miR-125a-5p: implications for cell migration in cervical tumor cells. *MicroRNA* 2018;**7**:54−61.
9. Hubaux R, Thu KL, Vucic EA, Pikor LA, Kung SH, Martinez VD, et al. Microtubule affinity-regulating kinase 2 is associated with DNA damage response and cisplatin resistance in non-small cell lung cancer. *Int J Cancer* 2015;**137**:2072−82.
10. Kato T, Satoh S, Okabe H, Kitahara O, Ono K, Kihara C, et al. Isolation of a novel human gene, *MARKL1*, homologous to *MARK3* and its involvement in hepatocellular carcinogenesis. *Neoplasia* 2001;**3**:4−9.
11. Magnani I, Novielli C, Fontana L, Tabano S, Rovina D, Moroni RF, et al. Differential signature of the centrosomal MARK4 isoforms in glioma. *Anal Cell Pathol* 2011;**34**:319−38.
12. Beghini A, Magnani I, Roversi G, Piepoli T, Terlizzi SD, Moroni RF, et al. The neural progenitor-restricted isoform of the *MARK4* gene in

19q13.2 is upregulated in human gliomas and overexpressed in a subset of glioblastoma cell lines. *Oncogene* 2003;**22**:2581−91.

13. Jenardhanan P, Mannu J, Mathur PP. The structural analysis of MARK4 and the exploration of specific inhibitors for the MARK family: a computational approach to obstruct the role of MARK4 in prostate cancer progression. *Mol Biosyst* 2014;**10**:1845−68.

14. Pardo OE, Castellano L, Munro CE, Hu Y, Mauri F, Krell J, et al. miR-515-5p controls cancer cell migration through MARK4 regulation. *EMBO Rep* 2016;**17**:570−84.

15. Heidary AE, Shiban A, Song S, Attisano L. MARK4 inhibits hippo signaling to promote proliferation and migration of breast cancer cells. *EMBO Rep* 2017;**18**:420−36.

16. Khan P, Rahman S, Queen A, Manzoor S, Naz F, Hasan GM, et al. Elucidation of dietary polyphenolics as potential inhibitor of microtubule affinity regulating kinase 4: *in silico* and *in vitro* studies. *Sci Rep* 2017;**7**:9470.

17. Aneja B, Khan NS, Khan P, Queen A, Hussain A, Rehman MT, et al. Design and development of isatin-triazole hydrazones as potential inhibitors of microtubule affinity-regulating kinase 4 for the therapeutic management of cell proliferation and metastasis. *Eur J Med Chem* 2019;**163**:840−52.

18. Parveen I, Khan P, Ali S, Hassan MI, Ahmed N. Synthesis, molecular docking and inhibition studies of novel 3-*n*-aryl substituted-2-heteroarylchromones targeting microtubule affinity regulating kinase 4 inhibitors. *Eur J Med Chem* 2018;**159**:166−77.

19. Ma YT, Yang Y, Cai P, Sun DY, Sánchez-Murcia PA, Zhang XY, et al. A series of enthalpically optimized docetaxel analogues exhibiting enhanced antitumor activity and water solubility. *J Nat Prod* 2018;**81**:524−33.

20. Li DJ, Tong J, Zeng FY, Guo M, Li YH, Wang H, et al. Nicotinic ACh receptor α7 inhibits PDGF-induced migration of vascular smooth muscle cells by activating mitochondrial deacetylase sirtuin 3. *Br J Pharmacol* 2019;**176**:4388−401.

21. Lv G, Sun D, Zhang J, Xie X, Wu X, Fang W, et al. Lx2-32c, a novel semi-synthetic taxane, exerts antitumor activity against prostate cancer cells *in vitro* and *in vivo*. *Acta Pharm Sin B* 2017;**7**:52−8.

22. Wang HB, Ma XJ, Ren SM, John K, Buolamwini JK, Yan C. A small-molecule inhibitor of MDMX activates p53 and induces apoptosis. *Mol Cancer Ther* 2011;**10**:69−79.

23. Ding MM, Wang HB, Qu CR, Xu FH, Zhu YM, Lv GY, et al. Pyrazolo [1,5-*a*] pyrimidine TRPC6 antagonists for the treatment of gastric cancer. *Cancer Lett* 2018;**432**:47−55.

24. Yang YT, Guan DK, Lei L, Lu J, Liu JQ, Yang GQ, et al. H6, a novel hederagenin derivative, reverses multidrug resistance *in vitro* and *in vivo*. *Toxicol Appl Pharmaco* 2018;**341**:98−105.

25. Zhang D, Xu Q, Wang N, Yang YT, Liu JQ, Yu GH, et al. A complex micellar system co-delivering curcumin with doxorubicin against cardiotoxicity and tumor growth. *Int J Nanomedicine* 2018;**13**:4549−61.

26. Sun SY, Du GY, Xue J, Ma JB, Ge MM, Wang HB, et al. PCC0208009 enhances the anti-tumor effects of temozolomide through direct inhibition and transcriptional regulation of indoleamine 2,3-dioxygenase in glioma models. *Int J Immunopathol Pharmacol* 2018;**32**:1−14.

27. Ostrom QT, Gittleman H, Xu J, Kromer C, Wolinsky Y, Kruchko C, et al. CBTRUS statistical report: primary brain and other central nervous system tumors diagnosed in the United States in 2009−2013. *Neuro Oncol* 2016;**18**:1−75.

28. Wang JL, Ma YF, Cooper MK. Cancer stem cells in glioma: challenges and opportunities. *Transl Cancer Res* 2013;**2**:429−41.

29. Katsetos CD, Reginato MJ, Baas PW, D'Agostino L, Legido A, Tuszyn SJ, et al. Emerging microtubule targets in glioma therapy. *Semin Pediatr Neurol* 2015;**22**:49−72.

30. Josiana GA, Ricardo PR, Leonardo BF, Carlos HT. Structure-based drug design of novel MARK-3 inhibitors in cancer. *Curr Bioact Comp* 2014;**10**:131−8.

31. Jonathan RA, Josiana GA, Joao GP, Carlton AT, Carlos HP. Ligand-based drug design of novel MARK-3 inhibitors in cancer. *Curr Bioact Comp* 2014;**10**:112−23.

32. Trinczek B, Ebneth A, Mandelkow EM, Mandelkow E. Tau regulates the attachment/detachment but not the speed of motors in microtubule-dependent transport of single vesicles and organelles. *J Cell Sci* 1999;**112**:2355−67.

33. Preuss U, Mandelkow EM. Mitotic phosphorylation of tau protein in neuronal cell lines resembles phosphorylation in Alzheimer's disease. *Eur J Cell Biol* 1998;**76**:176−84.

34. Rovina D, Fontana L, Monti L, Novielli C, Panini N, Sirchia SM, et al. Microtubule-associated protein/microtubule affinity-regulating kinase 4 (MARK4) plays a role in cell cycle progression and cytoskeletal dynamics. *Eur J Cell Biol* 2014;**93**:355−65.

35. Abbott NJ. Blood−brain barrier structure and function and the challenges for CNS drug delivery. *J Inherit Metab Dis* 2013;**36**:437−49.